

Feedback-induced interactive dynamics: unitary but dissipative evolution

Shuohang Wu¹ and Zi Cai^{1,2,*}

¹*Wilczek Quantum Center and Key Laboratory of Artificial Structures and Quantum Control, School of Physics and Astronomy, Shanghai Jiao Tong University, Shanghai 200240, China*

²*Shanghai Research Center for Quantum Sciences, Shanghai 201315, China*

The time evolution of a physical system is generally described by a differential equation, which can be solved numerically by adopting a difference scheme with space-time discretization. This discretization, as a numerical artifact, results in accumulated errors during evolution thus usually plays a negative role in simulations. In a quantum circuit, however, the “evolution time” is represented by the depth of the circuit layer, thus is intrinsically discrete. Hence, the discretization-induced error therein is not a numerical artifact, but a physical observable effect responsible for remarkable nonequilibrium phenomena absent in conventional quantum dynamics. In this paper, we show that the combination of measurement feedback and temporal discretization can give rise to a new type of quantum dynamics characterized by unitary but dissipative evolution. As a physical consequence of such interactive dynamics, we reveal a localization phenomenon that is fundamentally distinct from the well-established Anderson localization.

Introduction – Generally, a quantum computer is an synthetic quantum many-body system distinct from the quantum materials that naturally exist in a solid state or other natural systems in many aspects. For instance, quantum measurement and the resulting wavefunction collapse play a much more important role in the former. Introducing quantum measurement into many-body physics provides a new perspective to this field. For example, the competition between random measurements and unitary dynamics in quantum circuits could give rise to an entanglement transition absent in traditional quantum materials[1–13]. Furthermore, measurements could play positive roles in quantum systems if the measurement outcome could be fed back into the systems, causing an effect on subsequential evolution. Such interactive dynamics with a combination of quantum measurement and classical feedback, plays an important role in quantum optimization[14], cooling[15], and error correction[16], further incorporating the quantum many-body effect might result in intriguing phenomena such as the dynamic preparation of entangled quantum states[17–19], feedback-induced nonlinear quantum dynamics[20, 21] as well as nonequilibrium phases[22] and phase transitions[23].

Another important difference between a quantum computer (*e.g.* a quantum circuit) and a quantum material in nature, is that the “evolution time” in the former is represented by the depth of the quantum circuit layer, thus is intrinsically discrete. In contrast, the evolution in the latter is continuous, the temporal discretization is nothing but a mathematical technique transforming a differential equation into a difference one, which is solvable by a classical computer. Numerically, a difference scheme with a finite time interval inevitably leads to accumulated errors during the evolution, which could jeopardize the accuracy of long-time simulation. Moreover, as an artifact of discretization in classical simulations, the accumulated error significantly depends on the difference

scheme[24]. However, the time evolution in a quantum circuit is intrinsically discrete, thus the discretization-induced error is not a numerical artifact, but a physical reality which may act on a systems in a more active way as a source of searching for intriguing quantum dynamics absent in conventional quantum dynamics.

In this study, we propose a new type of quantum dynamics induced by combining measurement feedback and temporal discretization. This interactive dynamics resembles neither the unitary evolution in closed systems, nor the dissipative dynamics in open quantum systems. Even though the proposed quantum system is not coupled to a bath thus its evolution is unitary, its energy is dissipated due to the temporal discretization. As a concrete example, we study a one-dimensional (1D) quantum lattice model, where the local density is measured at each quantum circuit layer, then the outcome is fed back to the subsequent layer to modify its onsite chemical potential. This model exhibits a dissipative unitary evolution driving the system into a localized phase. Unlike the well-established Anderson localization[25], the localization in our model is not due to the quantum interference effect, instead it originates from the existence of extensive metastable states which act like attracting basins in real space.

The model and its physical realization – A quantum circuit is composed of a sequence of computational layers. We assume the operation by the n -th layer of the quantum circuit could be represented by a unitary operator $\hat{U}_n = e^{-iT\hat{H}_n}$, where T is a control parameter representing the time interval, and H_n is the effective Hamiltonian defined in a 1D lattice with length L :

$$\hat{H}_n = \sum_i [-J(\hat{c}_i^\dagger \hat{c}_{i+1} + h.c) - \mu_i^n \hat{n}_i] \quad (1)$$

where i and n denote the site and layer (time step) index respectively. \hat{c}_i (\hat{c}_i^\dagger) is the annihilation (creation) operator of the spinless fermion on site i and $\hat{n}_i = \hat{c}_i^\dagger \hat{c}_i$ (A

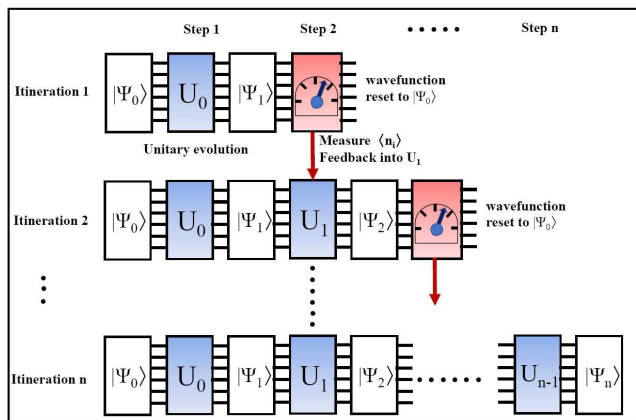


FIG. 1: (Color online) Schematic showing procedure for implementing the interactive dynamics in quantum circuit. Starting from an initial state $|\psi_0\rangle$, in iteration 1, we first operate \hat{U}_0 on $|\psi_0\rangle$ to derive $|\psi_1\rangle$, then measure its average local density and prepare \hat{U}_1 for next iteration. Finally, we reset the wavefunction to $|\psi_0\rangle$, and start iteration 2 following a similar procedure (deriving $|\psi_2\rangle$, measuring $\langle \hat{n}_i \rangle$ and preparing \hat{U}_2 , resetting the wavefunction to $|\psi_0\rangle$). We repeat this procedure until iteration n , at the end of which we realize a wavefunction $|\psi_n\rangle = \hat{U}_{n-1} \cdots \hat{U}_0 |\psi_0\rangle$.

spinless fermion in 1D lattice can be mapped to spin- $\frac{1}{2}$ qubit in a quantum circuit). J is the nearest-neighboring single-particle hopping amplitude and μ_i^n is the time-dependent onsite chemical potential. Starting from an initial state $|\psi_0\rangle$, the wavefunction at the n -th time step $|\psi_n\rangle$ after a sequence of unitary operations reads:

$$|\psi_n\rangle = \hat{U}_{n-1} \cdots \hat{U}_0 |\psi_0\rangle. \quad (2)$$

The feedback is introduced in a way that the on-site chemical potential in the n -th layer Hamiltonian is determined by the wavefunction of last layer $|\psi_{n-1}\rangle$ as:

$$\mu_i^n = \mu_i + V \langle \psi_{n-1} | \hat{n}_i | \psi_{n-1} \rangle \quad (3)$$

where μ_i is time-independent and randomly sampled from a uniform random distribution with $\mu_i \in [-\Delta, \Delta]$ and $\mu_i^0 = \mu_i$. The parameter V characterizes the strength of feedback.

To collect the information of local density, one needs to perform measurement after each time step (layer). However, these measurements will lead to wavefunction collapse, which has not been taken into account in the evolution defined in Eq.(2). To preserve the unitarity of the evolution and collect the information of the physical quantities in the meantime, we use an iterative feedback-based algorithm for quantum circuit[14] as illustrated in Fig.1. The basic idea is that after the n -th time step, we measure the physical quantities over the wavefunction $|\psi_n\rangle$ and prepare the evolution operator \hat{U}_n , then reset the wavefunction to the $|\psi_0\rangle$ and start over from

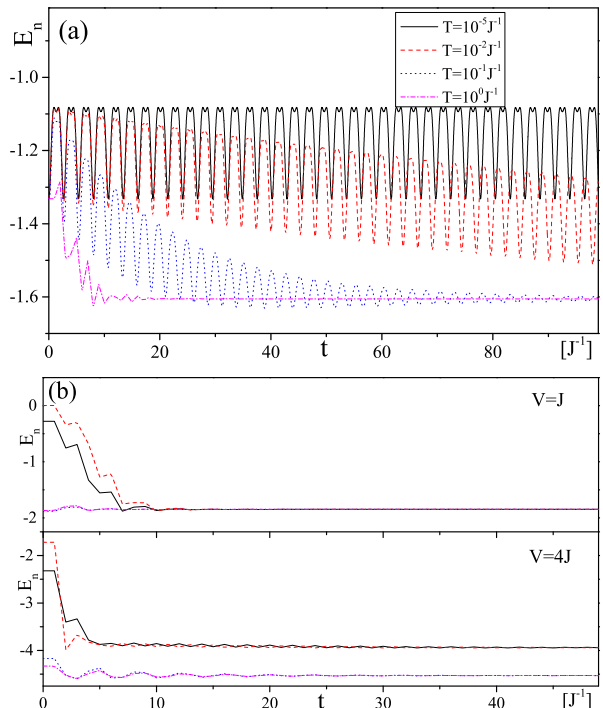


FIG. 2: (Color online) (a) Dynamics of the instantaneous energy E_n for an $L = 2$ system with different time intervals (T). Without losing generality, we assume $\mu_1 = -\mu_2 = \Delta/2$. The parameters are chosen as $V = J$, $\Delta = J$. (b) Dynamics of E_n starting from different initial states in the presence of a small $V = J$ with only one steady state (upper panel) and a large $V = 4J$ with two steady states (lower panel). Other parameters are chosen as $T = J^{-1}$ and $\Delta = 0.5J$.

beginning until it reaches the n -th layer again. We then operate the preliminarily prepared operator \hat{U}_n on $|\psi_n\rangle$ to obtain $|\psi_{n+1}\rangle$. Consequently, to obtain the wavefunction $|\psi_n\rangle$, one has to perform $\frac{n(n+1)}{2}$ unitary operations in total. In the following, we will analyze the consequence of this feedback-induced interactive dynamics.

The simplest albeit nontrivial case with $L = 2$ – We start with the simplest case of one particle in a two-site lattice. Despite its extreme simplicity, this model captures the most important ingredients of interactive dynamics in a quantum circuit: feedback-induced nonlinearity and discretization-induced dissipation. This simple model, with a Hilbert space dimension of 2, can be mapped to a spin- $\frac{1}{2}$ model with a time-dependent magnetic field whose strength and direction are, in turn, determined by the spin itself. In the continuous time limit ($T \rightarrow 0$), the equation of motion (EOM) of this model become a nonlinear differential equation taking the same form as the mean-field EOM of the Lipkin-Meshkov-Glick(LMG) model[26]. However, the physical origin of the nonlinearity in our model is feedback instead of interaction. Typically, this EOM exhibits persistent oscillation, which depends strongly on the initial

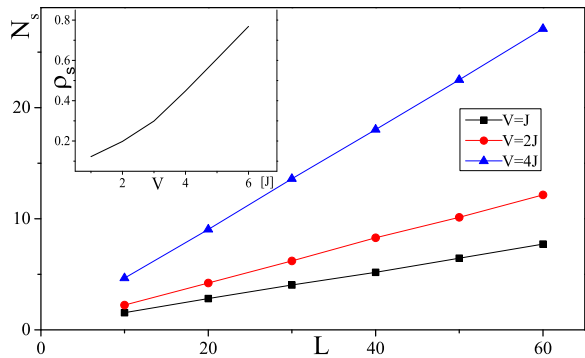


FIG. 3: (Color online) In a 1D lattice with length L , the total number of the steady state N_s as a function of L with different V , which exhibit a linear relation $N_s = \rho_s L$. The inset is the dependence of the steady state density ρ_s on V . $\Delta = 2J$.

state[27]. However, the intrinsic temporal discreteness (finite T) in the quantum circuit will introduce dissipation and qualitatively alter the long-time dynamics.

The instantaneous energy $E_n = \langle \psi_n | H_n | \psi_n \rangle$ as a function of evolution time $t = nT$ for different T , comprising a fixed V has been plotted in Fig.2 (a). After sufficiently long time, E_n keeps being dissipated for a finite T and approaches a minimum value corresponding to the ground state energy of the mean-field LMG model[27]. This energy dissipation is not due to the coupling to a bath, since the evolution in Eq.(2) is unitary. Instead, it is a reminiscence of the artificial dissipation induced by temporal discretization in the classical simulation of Hamiltonian dynamics, where this numerical artifact can be eliminated by choosing other difference schemes[24]. Different from the classical simulation, the “difference scheme” in our model has already been fixed by the iterative feedback-based procedure in the quantum circuit.

Subsequently, we fix T and check the dependence of long-time dynamics on the feedback parameter V . As shown in Fig.2 (b), for a small V , the long-time evolutions always converge to the same steady state irrespective of the initial states. However, when V exceeds a threshold, a new steady state with higher energy emerges, and the system could fall into either steady state depending on the initial state. It is worth emphasizing that these two steady states are not orthogonal with each other, and an arbitrary superposition of them is no longer steady due to the nonlinearity of the EOM. If V is further increased, more steady states will emerge. These steady states act as attracting basins for different initial states, and their structure can be understood without solving the time evolution[27]. These states are “steady” in the sense that they are robust against small perturbations imposed on them. However, a strong perturbation may drive the system out of the original basin, thus these steady states are actually “metastable”.

Single particle dynamics – Next, we generalize our discussions to the single-particle dynamics in a 1D lattice in the presence a static disordered and a dynamically modified chemical potential defined in Eq.(3). Using an iterative method combined with a stability analysis, we can enumerate all the steady states in such a 1D system. The wavefunctions of these single-particle steady states are spatially local, and their total number is proportional to the system size $N_s = \rho_s L$ as shown in Fig.3. For a fixed T , the dependence of the steady state density ρ_s on the feedback factor V is plotted in the inset of Fig.3. In the following, we will analyze the physical consequences of these steady states.

In the continuous time limit ($T \rightarrow 0$), the single-particle dynamics is described by a nonlinear differential equation, which takes the same form of a Gross-Pitaevskii (GP) equation[28], even though the nonlinear term therein has a different origin. The diffusion dynamics of a wavepacket governed by a GP equation in a 1D disordered lattice has been intensively studied[29, 30]. Similar to the $L = 2$ case, the temporal discretization with a finite T qualitatively changes the long-time dynamics of the continuous time limit. To illustrate this point, we consider an example of a small 1D system with only two steady states as shown in Fig.4 (a), and put one particle on the site with the highest μ_i (say $i = 6$), then study its dynamics starting from this initial state. The dynamics of the instantaneous energy E_n with different T is plotted in Fig.4 (b), from which we can find that for a small T , E_n keeps oscillating around its original value for a long time before starting to decay after a sufficiently long-time (the oscillation become persistent in the continuous time limit). For a larger T , E_n is quickly dissipated and approaches the energy of one of the steady states (steady state 1 centered around site 4).

The dynamics of the wavepacket can be seen more clearly by monitoring its center of mass (COM) defined as $C_n = \sum_i i \langle \psi_n | \hat{n}_i | \psi_n \rangle$. The dependence of the COM dynamics on the initial state is shown in Fig.4 (c), from which we can see that if a particle is injected into the system, it will be attracted and finally trapped by its nearby localized steady state, making it unable to propagate far away from its initial position. For a large V case where the steady state density $\rho_s \simeq 1$, almost every lattice site is centered by a localized steady state wavefunction, and a particle injected into the system will be localized around its original lattice site. As a result, the information of the initial position of the particle can be (partially) preserved in this interactive dynamics.

It is worthwhile to compare these phenomena with the well-established Anderson localization. Even though they share a lot of common properties such as the spatially localized wavefunction and the preservation of the initial state information, there are fundamental differences between them. For instance, while the Anderson localization originates from the interference effect of wave,

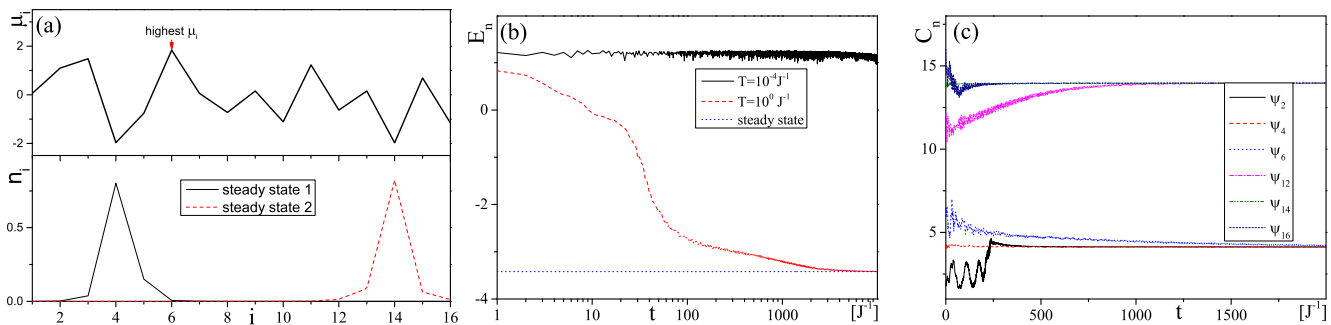


FIG. 4: (Color online) (a) An $L = 16$ 1D lattice with a set of random $\mu_i \in [-\Delta, \Delta]$ (upper panel) and the corresponding density distribution of the two single-particle steady states (lower panel), each of which is centered at lattice sites ($i = 4$ and 14) with the local minimum potential. (b) Dynamics of E_n starting from an initial state located on the lattice site ($i = 6$) with the maximum potential with different T . In the long-time limit, E_n will approach the energy of the steady state located on lattice site $i = 4$ (blue dashed line) (c) Dynamics of the center of mass C_n starting from different localized initial states (ψ_i indicates an initial state that the particle is located on site i). Depending on its initial position, the particle will finally fall into either steady state 1 or 2. Other parameters are chosen as $\Delta = 2J$, $V = J$ for (a)-(c) and $T = J^{-1}$ for (c).

while the localization in our model is due to the extensive metastable states, each acting as an attracting basin that traps nearby particles. This mechanism reminds us of the associative memory in the classical Hopfield model with a set of stored memory patterns[31]: when a given configuration is similar enough to one of them, the system can retrieve the correct stored pattern via a dissipative dynamics of classical annealing[32, 33]. Another difference between the Anderson localization and our model is that while the energy is conserved in the former, and there is no qualitative difference between the localized states on the bottom or on the top of the energy spectrum. This similarity between the low energy and high energy states does not hold in our model due to its intrinsic dissipative nature, where the localized steady states are usually at low energy.

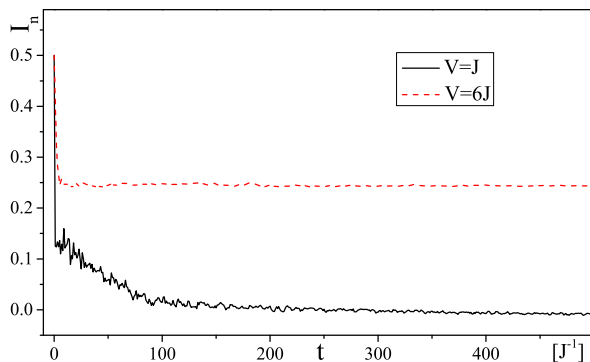


FIG. 5: (Color online) Dynamics of the initial state memory quantity I_n with different V in a half-filled many-body system. $T = J^{-1}$, $\Delta = 2$ and $L = 100$. The initial state is chosen as a random product state.

Many-body dynamics – Finally, we study the many-body dynamics in our model by considering the case with

half-filling. To assess the memory of the initial state information, we choose the initial state as a random product state $|\psi_0\rangle = |n_1 n_2 \dots n_L\rangle$ with n_i being randomly set as 0 or 1, which satisfies $\sum_i n_i = \frac{L}{2}$ (half-filling). After an n -step evolution defined in Eq.(2), the wavefunction turns out to be $|\psi_n\rangle$, from which we could then derive the average value of the local density $\tilde{n}_i = \langle \psi_n | \hat{n}_i | \psi_n \rangle$. To measure the difference between the density distributions of the initial and final states, we defined a quantity $I_n = \frac{1}{L} \sum_i (-1)^{n_i+1} \tilde{n}_i$, which will reach its maximum value of $\frac{1}{2}$ if $\tilde{n}_i = n_i \forall i$, and will approach zero in the thermodynamic limit if $\{\tilde{n}_i\}$ and $\{n_i\}$ are uncorrelated. Notice that for a special initial state $|\psi_0\rangle = |1010 \dots 10\rangle$, $I_n = \frac{1}{L} \sum_i (-1)^{i+1} \tilde{n}_i$ is the density imbalance between the even and odd sublattice, which has been widely used as an experimental signal of many-body localization[34]. As shown in Fig.5, for a large V , I_n converges to a finite value, indicating a memory of the position information of the initial state after a sufficiently long time. For a small V case with a low ρ_s , I_n decays to a small value close to zero, indicating that the position information of the initial state has been washed out during the evolution. We expect a crossover instead of a phase transition occurs between the small and large V cases, since $\rho_s(V)$ is an analytic function, as shown in the inset of Fig.3.

Discussion – To avoid misunderstanding of the temporal discretization, we should emphasize it does not mean the evolution time in our system has to be discrete, instead, it only requires the measurement and feedback to be performed at discrete time slices, thus the time-dependence of feedback quantities is a step-like function instead of a continuous one. This is the origin of dissipation in our system and makes it fundamentally distinct from the self-consistent mean-field dynamics. Consequently, the physical implementation of the proposed interactive dynamics is not only restricted to quantum

circuits, but can be realized in most synthetic quantum systems, as long as their physical quantities can be repeatedly measured during the evolution and Hamiltonian parameters can be dynamically manipulated according to the measurement outcomes. For instance, this localization dynamics is ready to be realized in current ultracold atomic setups in an optical lattice, where the local lattice potential can be dynamically modified. However, compared to other synthetic quantum systems, the initial state resetting is much more easier in quantum circuit.

Conclusion and outlook – In summary, we propose unitary but dissipative dynamics due to the interplay between feedback-induced nonlinearity and discretization-induced dissipation. As a physical consequence of this intriguing dynamics, a localization phenomenon distinct from Anderson localization has been uncovered. Future developments will include the generalization of these results to a genuinely open quantum system coupled to a bath, where the decoherence will make the evolution no longer unitary. This problem is particularly important for the quantum circuit setup, where decoherence is inevitable. We expect that the competition between the intrinsic dissipation in our system and the heating by external noise may give rise to interesting nonequilibrium phases and phase transitions. Furthermore, the interplay between the quantum many-body effect and interactive dynamics may give rise to intriguing non-equilibrium quantum matter in a genuine interacting quantum system. Lastly, by designing other feedback protocols, it is possible to realize various symmetry breaking phases (*e.g.* non-equilibrium superconductor) or even more exotic quantum phases (*e.g.* spin liquid) as the steady state of such an interactive quantum system.

Acknowledgments.—ZC acknowledges helpful discussion with S.Jin and Z.X.Guo. This work is supported by the National Key Research and Development Program of China (Grant No. 2020YFA0309000), NSFC of China (Grant No.12174251), Natural Science Foundation of Shanghai (Grant No.22ZR142830), Shanghai Municipal Science and Technology Major Project (Grant No.2019SHZDZX01).

* Electronic address: zcai@sjtu.edu.cn

- [1] B. Skinner, J. Ruhman, and A. Nahum, *Phys. Rev. X* **9**, 031009 (2019).
- [2] Y. Li, X. Chen, and M. P. A. Fisher, *Phys. Rev. B* **98**, 205136 (2018).
- [3] Y. Li, X. Chen, and M. P. A. Fisher, *Phys. Rev. B* **100**, 134306 (2019).
- [4] X. Cao, A. Tilloy, and A. D. Luca., *SciPost Phys.* **7**, 024 (2019).
- [5] Y. Bao, S. Choi, and E. Altman, *Phys. Rev. B* **101**, 104301 (2020).
- [6] C.-M. Jian, Y.-Z. You, R. Vasseur, and A. W. W. Ludwig, *Phys. Rev. B* **101**, 104302 (2020).
- [7] M. J. Gullans and D. A. Huse, *Phys. Rev. X* **10**, 041020 (2020).
- [8] X. Chen, Y. Li, M. P. A. Fisher, and A. Lucas, *Phys. Rev. Research* **2**, 033017 (2020).
- [9] A. Zabalo, M. J. Gullans, J. H. Wilson, S. Gopalakrishnan, D. A. Huse, and J. H. Pixley, *Phys. Rev. B* **101**, 060301 (2020).
- [10] X. Turkeshi, R. Fazio, and M. Dalmonte, *Phys. Rev. B* **102**, 014315 (2020).
- [11] A. Lavasani, Y. Alavirad, , and M. Barkeshli., *Nature Physics* **17**, 342 (2021).
- [12] M. Buchhold, Y. Minoguchi, A. Altland, and S. Diehl, *Phys. Rev. X* **11**, 041004 (2021).
- [13] M. Ippoliti, M. J. Gullans, S. Gopalakrishnan, D. A. Huse, and V. Khemani, *Phys. Rev. X* **11**, 011030 (2021).
- [14] A. B. Magann, K. M. Rudinger, M. D. Grace, and M. Sarovar, *arXiv e-prints arXiv:2103.08619* (2021), 2103.08619.
- [15] E. P. Yamaguchi, H. M. Hurst, and I. B. Spielman, *arXiv e-prints arXiv:2206.04156* (2022), 2206.04156.
- [16] B. M. Terhal, *Rev. Mod. Phys.* **87**, 307 (2015).
- [17] H. M. Hurst, S. Guo, and I. B. Spielman, *Phys. Rev. Research* **2**, 043325 (2020).
- [18] L.-N. Wu and A. Eckardt, *Phys. Rev. Research* **4**, L022045 (2022).
- [19] J. Y. Lee, W. Ji, Z. Bi, and M. P. A. Fisher, *arXiv e-prints arXiv:2208.11699* (2022), 2208.11699.
- [20] S. Lloyd and J.-J. E. Slotine, *Phys. Rev. A* **62**, 012307 (2000).
- [21] M. H. Muñoz Arias, P. M. Poggi, P. S. Jessen, and I. H. Deutsch, *Phys. Rev. Lett.* **124**, 110503 (2020).
- [22] M. McGinley, S. Roy, and S. A. Parameswaran, *Phys. Rev. Lett.* **129**, 090404 (2022).
- [23] D. A. Ivanov, T. Y. Ivanova, S. F. Caballero-Benitez, and I. B. Mekhov, *Phys. Rev. Lett.* **124**, 010603 (2020).
- [24] K. Feng, *Journal of Computational Mathematics* **4**, 279 (1985).
- [25] P. W. Anderson, *Phys. Rev.* **109**, 1492 (1958).
- [26] H. J. Lipkin, N. Meshkov, and A. J. Glick, *Nucl. Phys.* **62**, 188 (1965).
- [27] See the supplementary material for the details of the mean-field dynamics of the Lipkin-Meshkov-Glick model as well as an analysis of its stationary states and their stability. As a comparison, we also studied the single-spin interactive dynamics with finite time interval, which does not only change the structure of the stationary states, but also qualitatively alters their stabilities.
- [28] L. Pitaevskii and S. Stringari, *Bose-Einstein Condensation* (Clarendon, Oxford, 2003, 2003).
- [29] A. S. Pikovsky and D. L. Shepelyansky, *Phys. Rev. Lett.* **100**, 094101 (2008).
- [30] B. Shapiro, *Phys. Rev. Lett.* **99**, 060602 (2007).
- [31] J. J. Hopfield, *PNAS* **79**, 2554 (1982).
- [32] D. J. Amit, H. Gutfreund, and H. Sompolinsky, *Phys. Rev. Lett.* **55**, 1530 (1985).
- [33] D. J. Amit, H. Gutfreund, and H. Sompolinsky, *Phys. Rev. A* **32**, 1007 (1985).
- [34] M. Schreiber, S. S. Hodgman, P. Bordia, H. P. Luschen, M. H. Fischer, R. Vosk, E. Altman, U. Schneider, and I. Bloch, *Science* **349**, 842 (2015).

Supplementary material

In this supplementary material, we first analyze the mean-field dynamics of the Lipkin-Meshkov-Glick model, which is equivalent to the $L = 2$ case in our model in the continuous time limit. The stationary states as well as their stability have been investigated analytically. In the second section, we focus on the interactive dynamics of our model with $L = 2$, and show that the temporal discretation does not only change the structure of the stationary states, but also qualitatively alters their stabilities.

MEAN-FIELD DYNAMICS OF LIPKIN-MESHKOV-GLICK MODEL

In this section, we analyze the mean-field dynamics of the Lipkin-Meshkov-Glick (LMG) model, which is equivalent to the $L = 2$ case in our model in the maintext in the continuous time limit ($T \rightarrow 0$).

The LMG model describes an interacting quantum many-body system composed of a set of $s = \frac{1}{2}$ spins with all-to-all interaction, whose Hamiltonian reads:

$$H_s = -\frac{V}{N} \sum_{kk'} \hat{s}_k^z \hat{s}_{k'}^z - \sum_k 2[J\hat{s}_k^x + \Delta\hat{s}_k^z] \quad (4)$$

where \hat{s}_k^α is the spin- $\frac{1}{2}$ operator operating on k th site(mode) defined as $\hat{s}_k^\alpha = \frac{1}{2}\hat{\sigma}_k^\alpha$ ($\hat{\sigma}_k^\alpha$ are the three Pauli matrices with $\alpha = x, y, z$). 2Δ ($2J$) is the strength of a uniform magnetic field along $z(x)$ -direction. N is the total number of spins and the $\frac{1}{N}$ pre-factor in Eq.(4) guarantees that the total interacting energy scales linearly with N . J is the strength of the all-to-all interaction that is spatially uniform.

A mean-field treatment

In the thermodynamic limit $N \rightarrow \infty$, due to the all-to-all feature, the interaction terms in Eq.(4) can be decoupled by introducing a mean-field time-dependent ferromagnetic order parameters

$$s(t) = \frac{1}{N} \sum_k \langle \psi(t) | \hat{s}_k^z | \psi(t) \rangle \quad (5)$$

with $|\psi(t)\rangle$ representing the wavefunction of the system at time t . Since the Hamiltonian for all k -mode are identical, we omit the subscript k in the following. The mean-field(MF) Hamiltonian turns to a set of spin- $\frac{1}{2}$ systems as $\tilde{H}_s(t) = N\tilde{H}(t)$ with :

$$\tilde{H}(t) = -[2Vs(t) + 2\Delta]\hat{s}^z - 2J\hat{s}^x, \quad (6)$$

and the corresponding equation of motion(EOM) reads:

$$i \frac{d}{dt} |\psi\rangle = \tilde{H}(t) |\psi\rangle \quad (7)$$

where the wavefunction $|\psi(t)\rangle = [\alpha(t), \beta(t)]^T$.

Stationary states

We first analyze the stationary state $|\psi_s^*\rangle$ of Eq.(7), which corresponds to the eigenstates of Eq.(6) with a time-independent $s(t) = s^*$ that can be solved self-consistently. For instance, one of stationary state is the MF groundstate of \tilde{H} , where the corresponding MF order parameter s_1^* can be solved via the self-consistent MF equation:

$$2s_1^* = \frac{Vs_1^* + \Delta}{\sqrt{[Vs_1^* + \Delta]^2 + J^2}} \quad (8)$$

and the corresponding MF ground state energy is

$$E_G = -\sqrt{[Vs_1^* + \Delta]^2 + J^2} + V(s_1^*)^2 \quad (9)$$

which agrees with the asymptotic value of E_n in the dissipative dynamics of $L = 2$ case with small V as shown in Fig.2 (a) the maintext. This indicates that the steady state in this $L = 2$ case with small V is indeed the MF ground state of the LMG model.

We consider a special case with $\Delta = 0$, where the Hamiltonian.(4) preserves the Z_2 symmetry ($s_k^z \rightarrow -s_k^z$). In this case, we can solve Eq.(8) analytically. For $V < 2J$, there is only one solution $s_1^* = 0$, while for $V > 2J$, besides the trivial $s_1^* = 0$ solution, two new solutions $s_1^* = \pm \frac{1}{2} \sqrt{1 - (\frac{2J}{V})^2}$ emerge, each of which correspond to a Z_2 symmetry breaking phase. Even though the Hamiltonian.(6) is a single-spin system, it is an MF description of an infinite dimensional interacting system, thus can exhibit spontaneous symmetry breaking.

One can derive the other stationary state using a similar self-consistent procedure, where we choose the highest eigenstate instead of the groundstate. The MF order parameter s_2^* in this case satisfies the equation:

$$2s_2^* = -\frac{Vs_2^* + \Delta}{\sqrt{[Vs_2^* + \Delta]^2 + J^2}} \quad (10)$$

Stability analysis

One crucial difference between the stationary states in our model and the equilibrium states is that our model is a dynamical model, thus the stability of these stationary states is an important issue. Let $|\psi^*\rangle = [\alpha^*, \beta^*]^T$ be one of the steady state wavefunctions with the MF order parameter s^* . To analyze its stability under the EOM.(7), we prepare an initial state that slight deviates from the steady state wavefunction as $|\psi'\rangle = [\alpha^* + \delta\alpha, \beta^* + \delta\beta]^T$, and study the evolution of these small deviations $|\delta\psi\rangle =$

$[\delta\alpha, \delta\beta]^T$. By substituting $|\psi'\rangle$ into EOM.(7), and ignoring the higher order terms of $\delta\alpha$ and $\delta\beta$, we can derive a linearized EOM for $|\delta\psi\rangle$ as:

$$\frac{d}{dt}|\delta\psi\rangle = \mathbb{M}(s^*)|\delta\psi\rangle \quad (11)$$

where $\mathbb{M}(s^*)$ is a time-independent 2×2 linearized matrix depending on s^* . For instance, for $\Delta = 0$, if we expand around the trivial steady state $s_1^* = 0$, $\mathbb{M}(s_1^*)$ reads:

$$\mathbb{M}(s_1^*) = -i \begin{pmatrix} 0 & 2J \\ 2J & 0 \end{pmatrix}, \quad (12)$$

whose eigenvalues are purely imaginary, which indicates a marginal stable stationary state where the small deviation around it neither diverges to infinity, nor converges to zero during the time evolution. Instead, they exhibit persistent oscillations within a finite regime of the phase space. Notice that this result is irrespective of the value of V , and can apply for both the symmetry breaking ($V > 2J$) and unbreaking phases ($V < 2J$).

More generally, one can check this situations with other parameters (*e.g.* $\Delta \neq 0$), and other steady states (*e.g.* s_2^*), and the result is qualitatively the same. Physically, this is due to the fact that the original LMG Hamiltonian.(4) is time-independent, thus is a conserved system. However, this conservation only holds in this continuous time case, as we will show in the subsequential section.

FEEDBACK-INDUCED INTERACTIVE QUANTUM DYNAMICS FOR A SINGLE SPIN: EFFECT OF TEMPORAL DISCRETIZATION

Now we consider the interactive quantum dynamics in our model. As stated in the maintext, the $L = 2$ case of our model is equivalent to a single spin system, whose evolution is divided into n steps, each of which is characterized by an effective Hamiltonian H_n and a time interval T . To compare it to the MF dynamics of the LMG model discussed above, we adopt the spin language, in which the evolution can be expressed as:

$$|\psi_n\rangle = e^{-iH_{n-1}T} \dots e^{-iH_1T} e^{-iH_0T} |\psi_0\rangle \quad (13)$$

where

$$H_n = -[2Vs_{n-1}^z + 2\Delta]\hat{s}^z - 2J\hat{s}^x, \quad (14)$$

where $s_{n-1}^z = \langle \psi_{n-1} | \hat{s}^z | \psi_{n-1} \rangle$. Notice H_n takes a similar form of Eq.(6), where the self-consistent order parameter $s(t)$ is replaced by the averaged value of \hat{s}^z obtained by the measurement in the end of last time step. In the limit $T \rightarrow 0$, the dynamics is reduced to the MF dynamics of the LMG model studied above. In the following, we will show that a finite T qualitatively changes not only the structure of the stationary states, but also their stability.

Stationary states

The evolution of the wavefunction in the discrete time step can be expressed in terms of an iternate formula as:

$$|\psi_n\rangle = e^{-iH_{n-1}T} |\psi_{n-1}\rangle \quad (15)$$

where $|\psi_n\rangle = [\alpha_n, \beta_n]^T$. The evolution operator can be expressed as:

$$e^{-iH_nT} = \begin{pmatrix} \cos \gamma_n T + i \frac{\tilde{\Delta}_n}{\gamma_n} \sin \gamma_n T & i \frac{J}{\gamma_n} \sin \gamma_n T \\ i \frac{J}{\gamma_n} \sin \gamma_n T & \cos \gamma_n T - i \frac{\tilde{\Delta}_n}{\gamma_n} \sin \gamma_n T \end{pmatrix}, \quad (16)$$

where $\tilde{\Delta}_n = Vs_{n-1}^z + \Delta$, and $\gamma_n = \sqrt{\tilde{\Delta}_n^2 + J^2}$.

Since a wavefunction multiplied by a overall phase factor doesn't change any physical observable quantity, a stationary wavefunction $|\psi_n^*\rangle$ in such a discrete time evolution satisfies $|\psi_n^*\rangle = e^{i\delta} |\psi_{n-1}^*\rangle$ and $s_n^z = s_{n-1}^z = s^*$, which in turn indicates that $|\alpha_n/\beta_n| = |\alpha_{n-1}/\beta_{n-1}|$. Using this identity, we can derive the stationary state condition as:

$$(J\eta^2 - 2\tilde{\Delta}\eta - J) \sin(\gamma T) = 0 \quad (17)$$

where

$$\begin{aligned} \eta &= \pm \sqrt{\frac{1+2s^*}{1-2s^*}} \\ \tilde{\Delta} &= \Delta + Vs^* \\ \gamma &= \sqrt{J^2 + \tilde{\Delta}^2} \end{aligned}$$

According to the stationary condition in Eq.(17), there are two types of stationary states. The first is characterized by the solutions of $J\eta^2 - 2\tilde{\Delta}\eta - J = 0$, which are independent on the time interval T . These stationary solutions of the order parameters are the same with the ones derived in the continuous time limit discussed previously (s_1^* and s_2^*), which indicates that the stationary states in the continuous time limit are also the stationary states under the discrete time evolution. However, their stability against small perturbations are different, as we will show latter on.

One of the most remarkable consequence of the temporal discretization is that it leads to a new type of stationary states absent in the continuous time limit, which are characterized by the solutions of $\sin \gamma T = 0$. More specifically, this condition turns to

$$(\Delta + Vs^*)^2 = \left(\frac{m\pi}{T}\right)^2 - J^2 \quad (18)$$

where m is an integer. The solution of Eq.(18) can be expressed as:

$$s_m^* = \frac{1}{V} \left[\pm \sqrt{\left(\frac{m\pi}{T}\right)^2 - J^2} - \Delta \right] \quad (19)$$

Notice $|s_m^*| \leq \frac{1}{2}$ according to its definition, thus the solution of Eq.(19) does not necessarily exist for an arbitrary V . For instance, for the case with $\Delta = 0$, the minimum value of the right side of Eq.(19) is $\frac{1}{V} \sqrt{(\frac{\pi}{T})^2 - J^2}$, which takes place at $m = 1$, while the maximum value of the left side of Eq.(19) is $\frac{1}{2}$. Therefore, there is no solution for Eq.(19) if V is smaller than a critical value $V_c = 2\sqrt{(\frac{\pi}{T})^2 - J^2}$. If V is further increased, more and more solutions emerge correspond to different values of the integer m . This agrees with the numerical results as shown the $L = 2$ case in the maintext.

Stability analysis

In general, it is difficult to analytically study the stability of the stationary states. To this end, we focus on the simplest case with $\Delta = 0$, which allows us to analyze the stability of the stationary state with $s_1^* = 0$ analytically, and show how it is qualitatively changed by the temporal discretization. The time evolution of the wavefunction at discrete time steps can be described by the iteration relation:

$$\begin{pmatrix} \alpha_{n+1} \\ \beta_{n+1} \end{pmatrix} = e^{-iH_n T} \begin{pmatrix} \alpha_n \\ \beta_n \end{pmatrix}, \quad (20)$$

where the evolution operator $e^{-iH_n T}$ is defined as in Eq.(16). For a stationary state with $\Delta = 0$ and $s^* = 0$, its wavefunction can be expressed as $|\psi^*\rangle = [\frac{1}{\sqrt{2}}, \frac{1}{\sqrt{2}}]^T$.

To study the stability of this stationary state, we impose a small perturbation on this wavefunction $|\psi\rangle = [\frac{1}{\sqrt{2}} + \delta\alpha, \frac{1}{\sqrt{2}} + \delta\beta]^T$, where the corresponding order parameter in Eq.(16) turns to be $s = \sqrt{2}[(\delta\alpha - \delta\beta) + (\delta\alpha)^2 - (\delta\beta)^2]$ (we assume both $\delta\alpha$ and $\delta\beta$ are real for simplicity). After the one-step evolution defined in Eq.(20), the wavefunction becomes $|\psi'\rangle = [\frac{1}{\sqrt{2}} + \delta\alpha', \frac{1}{\sqrt{2}} + \delta\beta']^T$. By substituting the s into H_n , expanding Eq.(20) in terms of $\delta\alpha$ and $\delta\beta$ and only keeping the linear terms of them, one can derive a linear relationship between $[\delta\alpha, \delta\beta]^T$ and $[\delta\alpha', \delta\beta']^T$ as:

$$\begin{pmatrix} \delta\alpha' \\ \delta\beta' \end{pmatrix} = \mathbb{J} \begin{pmatrix} \delta\alpha \\ \delta\beta \end{pmatrix}, \quad (21)$$

where \mathbb{J} is the Jacobian matrix of the iteration transformation, which is defined as:

$$\mathbb{J} = \begin{pmatrix} \frac{\partial \delta\alpha'}{\partial \delta\alpha} & \frac{\partial \delta\alpha'}{\partial \delta\beta} \\ \frac{\partial \delta\beta'}{\partial \delta\alpha} & \frac{\partial \delta\beta'}{\partial \delta\beta} \end{pmatrix} = \begin{pmatrix} \cos \mathbf{t} + \frac{iV}{2J} \sin \mathbf{t} & i(1 - \frac{V}{2J}) \sin \mathbf{t} \\ i(1 - \frac{V}{2J}) \sin \mathbf{t} & \cos JT + \frac{iV}{2J} \sin \mathbf{t} \end{pmatrix},$$

where the dimensionless parameter $\mathbf{t} = JT$ is proportional to the time interval T .

The stability of iteration defined in Eq.(21) depends on the eigenvalues of the Jacobian matrix \mathbb{J} :

$$\begin{aligned} \lambda_1 &= \cos \mathbf{t} + i \sin \mathbf{t} \\ \lambda_2 &= \cos \mathbf{t} + i(\frac{V}{J} - 1) \sin \mathbf{t} \end{aligned}$$

Notice that $|\lambda_1| = 1$ irrespective of the value of V and T , thus the stability is crucially determined by the value of $|\lambda_2|$, which reads:

$$|\lambda_2| = \sqrt{1 + \sin^2 JT [(V/J)^2 - 2V/J]} \quad (22)$$

We first focus on the continuous time limit ($T \rightarrow 0$), in this case, $|\lambda_1| = |\lambda_2| = 1$, which indicates that the deviations $\delta\alpha$ and $\delta\beta$ neither diverge, nor converge under the evolution defined in Eq.(21), which reproduces the results discussed in the last section. For any finite T , Eq.(22) indicates that $|\lambda_2| < 1$ for $V < 2J$ indicates this stationary state with $s^* = 0$ is stable in this case ($\delta\alpha$ and $\delta\beta$ will converge to zero). On the contrary, for $V > 2J$, $|\lambda_2| > 1$ thus this stationary state is unstable. Notice that this is qualitatively different from the case in the continuous time limit, where the $s^* = 0$ solution is marginal stable irrespective of the value of V .

This difference is due to the temporal discretization-induced dissipation in our model, which will drive the system to the MF groundstate. As we analyzed in last section, for $V < 2J$, the stationary state with $s_1^* = 0$ is the MF groundstate, thus is stable against perturbation. For $V > 2J$, $s_1^* = 0$ state is still a stationary state, but no longer the groundstate. Instead, it is a local maximum in the energy landscape, and a small perturbation will drive it to the lower-energy symmetry breaking stationary states with $s_1^* = \pm \frac{1}{2} \sqrt{1 - (\frac{2J}{V})^2}$. In principle, one can analyze the stability of other stationary states (*e.g.* $s = s_2^*$ or $s = s_m^*$) following the similar procedure. Even though it may be difficult to derive an analytic formalism, one can always derive the Jacobian matrix as well as its eigenvalues numerically.